Chemical Physics Letters 587 (2013) 45–49

Contents lists available at ScienceDirect

Chemical Physics Letters

journal homepage: www.elsevier.com/locate/cplett

Facile synthesis of cuprous oxide nanooctahedra using electrodeless deposition

Feiyu Diao, Qingtian Du, Chunyan Li, Lei Shang, Yiqian Wang *

The Cultivation Base for State Key Laboratory, Qingdao University, No. 308 Ningxia Road, Qingdao 266071, PR China

ARTICLE INFO

Article history:
Received 17 August 2013
In final form 18 September 2013
Available online 25 September 2013

ABSTRACT

A facile electrodeless deposition method was developed for the preparation of cuprous oxide (Cu_2O) nanooctahedra by immersing different metal substrates with patterns or scratches on surface into a solution consisting of cupric sulphate ($CuSO_4$) and lactic acid (LA). Scanning electron microscopy (SEM) and transmission electron microscopy (TEM) examinations show that the formation of Cu_2O nanooctahedra is attributed to the reducibility of metal substrates. Cu_2O nanooctahedra can form only when the reducibility of metal substrates is more active than that of Cu. The optical properties and photocatalytic activity of Cu_2O nanooctahedra were also investigated.

1. Introduction

Cuprous oxide (Cu_2O), as a typical *p*-type semiconductor with a direct band gap of ~2.17 eV, is one of the few semiconductors that can be excited by visible light. Recently, visible-light photocatalysts have attracted increasing attention because they are widely used in the development and utilization of solar energy [1–4]. In addition, Cu_2O nanoparticles can also be used for photodegradation of water, photoelectric conversion materials, and negative electrode materials for lithium ion batteries [5,6]. Unique properties of nanostructured crystals are associated with both the size and the shape because they dictate the interfacial atomic arrangement of the nanomaterials [7,8]. Typically, the photocatalytic ability is dependent on the shape of Cu_2O nanocrystals [9,10]. It has been reported that Cu_2O nanooctahedra show better photocatalytic activity than Cu_2O nanocubes because {1 1 1} facets are more active than {1 0 0} facets [9]. As a result, novel and facile methods to fabricate Cu_2O nanocrystals with different morphologies have been of great research interest. To date, some progress has been made in the synthesis of Cu_2O nanocrystals with different shapes such as nanowires [11], multipods [12], nanobelts [13], nanocubes [14] and nanooctahedra [15,16]. Particularly, extensive studies have focused on the fabrication of Cu_2O nanooctahedra. For example, electrochemical deposition method [15] and surfactant aqueous phase method [17] have been used to fabricate Cu_2O nanooctahedra. Although different methods have been developed for the preparation of Cu_2O nanooctahedra, most of them are complicated and difficult because multiple additives are required. Currently, few reports can be found concerning a convenient way to prepare well-defined Cu_2O nanooctahedra with high uniformity. In addition, no detailed investigation has been carried out to clarify the formation mechanism of Cu_2O nanooctahedra.

In this Letter, electrodeless deposition was presented to prepare Cu_2O nanooctahedra. Electrodeless deposition is a type of redox reaction, which does not require a direct current voltage injection and any kind of additives. Uniform Cu_2O nanooctahedra with an average edge length of 150 ± 30 nm have been successfully fabricated. Based on the experimental results, a possible formation mechanism has been proposed. Furthermore, the optical properties and photocatalytic activity of Cu_2O nanooctahedra were studied.

2. Experimental details

First, we prepare a solution composed of 0.4 M cupric sulfate ($CuSO_4$) and 3 M LA. LA complexes with Cu^{2+} ions to stabilize them in alkaline solution and also subtly determines the morphology of final products as a face selective adsorption additive. Sodium hydroxide (NaOH) solution (4 M) is dropped into the solution under constant stirring. In this way, the pH of the solution is adjusted to 9, and the color will change from sky-blue to dark blue. The temperature of the solution is kept at 60 °C by immersing the beaker in a water bath. The Al foil with patterns or scratches on its surfaces was rinsed several times with acetone and deionized water. Subsequently the Al foils were immersed into the reaction mixture solution for 30 min and Cu_2O nanooctahedra were produced on the surface of Al foils. Three different metals (Fe, Cu and Pt) were also used as substrates to study the growth rate of Cu_2O nanooctahedra on different metal substrates. Finally, Cu_2O nanooctahedra were washed with deionized water several times to remove the reaction mixture. The as-deposited Cu_2O nanooctahedra were characterized using JEOL JEM2100F transmission electron microscope (TEM) operating at 200 kV and Hitachi S4800 scanning electron microscope (SEM).

---

* Corresponding author.
E-mail address: yqwang@qdu.edu.cn (Y. Wang).

0009-2614/$ - see front matter © 2013 Elsevier B.V. All rights reserved.
http://dx.doi.org/10.1016/j.cplett.2013.09.048

For measuring the optical properties of Cu_2O nanooctahedra, they were scraped off the Al substrates and dispersed into a mixture of ethanediol and water (volume ratio 1:1) to form a homogeneous suspension. The UV–vis absorption spectra were recorded on a TU 1909 UV–vis spectrophotometer.

Methyl orange (MO) was used as a pollutant to investigate the photocatalytic efficiency of Cu_2O nanooctahedra. Considering that Cu_2O nanooctahedra are deposited on Al foils, we immerse the Al foils with dimensions of 1×2 cm^2 into 5 mL MO solution with a concentration of 15 mg/L. Solutions were constantly stirred in the dark for 5 h before being irradiated by a 500 W xenon lamp equipped with a UV cutoff filter ($\lambda \geqslant 400$ nm) for 3 h at room temperature. The orange color of the MO solution gradually diminishes under the visible light irradiation in the presence of Cu_2O nanooctahedra indicating the degradation of MO. The MO concentration was analyzed by UV–vis absorption spectra.

3. Results and discussion

Figure 1a shows the full view of regular pattern on the surface of Al substrate. The pattern of QDU provides a template for the nucleation and growth of nanocrystals. Figure 1b shows the SEM image of the region enclosed by a square in Figure 1a. In Figure 1b, it can be found that most aggregations and particles gather together inside the kerfs of the patterns with only a few outside. A low-magnification SEM image of as-deposited nanoparticles is shown in Figure 1c, from which it can be seen that the shape of all particles is a regular octahedron. Analysis of more than 100 nanoparticles shows that the edge length of the octahedra ranges from 130 to 180 nm. Interestingly, the Cu_2O nanoparticles grew predominantly where the Al was scratched just prior to exposure to NaOH. In addition, their growth orientations are slightly tilted in random directions. Closer examination of the SEM image shows that the scratched areas of the Al substrate surface are covered with pores which might be due to the corrosive effects of the alkaline solution. Enlarged SEM images of Cu_2O nanooctahedron viewed from the top and side are shown in Figure 1d. They all look like a pyramid viewed from the top and a rhombus from the side, proving that these particles are perfect octahedron enclosed by eight {1 1 1} planes.

The morphology and microstructure of Cu_2O nanooctahedra were further characterized using TEM. Figure 2a shows a typical TEM image taken from an individual octahedron. Figure 2b shows a typical HRTEM image of the region enclosed by a square in Figure 2a. The interplanar spacing is measured to be 2.21 Å, which corresponds to the {0 0 2} crystal plane of Cu_2O. The corresponding SAED pattern viewed from [0 1 1] zone-axis shown in the inset indicates that it is single crystalline. The diffraction spots can be indexed using the lattice parameters of Cu_2O ($a = 4.2696$ Å).

To disclose the formation mechanism of Cu_2O nanooctahedra, the microstructure of the products deposited on different substrates was investigated. Four different metals, Al, iron (Fe), copper (Cu) and platinum (Pt), were used as substrates and the other conditions (pH, temperature, and solution concentrations) were kept the same during the experiments.

Figure 3a–d show SEM images of Cu_2O nanocrystals fabricated on different substrates by electrodeless deposition. Figure 3a shows a typical SEM image of Cu_2O nanocrystals on Al substrate, from which monodispersed Cu_2O nanooctahedra with an average edge length of 150 ± 30 nm can be seen. When Al is replaced with Fe, a solid and continuous film composed of many nanooctahedra on the surface of Fe substrate, as shown in Figure 3b. The dimensions are determined to be 111 ± 37 nm from statistical analysis of more than 100 nanooctahedra in the SEM images. Therefore, Cu_2O nanooctahedra grow faster on Fe than Al. Cu_2O nanooctahedra can also be obtained on the Cu substrate (Figure 3c). However, compared with Al substrate, fewer and smaller nanoparticles can be found on Cu surface without pores or netted texture. By analyzing more than 100 nanooctahedra, the average edge length of the nanooctahedra on Cu substrate is 130 ± 16 nm. This indicates that Cu_2O nanooctahedra grow faster on Al than Cu. If Pt was used as the substrate (Figure 3d), no Cu_2O nanocrystals formed. As we all know that the work function is the minimum amount of energy required to remove an electron from the surface of a metal. The higher the work function is, the weaker the reducibility of the metal is. The work functions for the different metal substrates are $\varphi_{Al} = 4.28$ eV, $\varphi_{Fe} = 4.5$ eV, $\varphi_{Cu} = 4.65$ eV and $\varphi_{Pt} = 5.65$ eV [18], therefore the reducibility of different metal substrates can be determined to be Al > Fe > Cu > Pt. From the above experimental results, it can be concluded that the growth rate of Cu_2O nanooctahedra depends on the reducibility of the metal substrate. The higher reducibility metal substrate has, the faster Cu_2O nanooctahedra growth rate (except for Al substrate) is. This is due to the dense and compact Al oxide film covered on the regions of Al surface without scratch, which can not be dissolved by NaOH. In order to certify

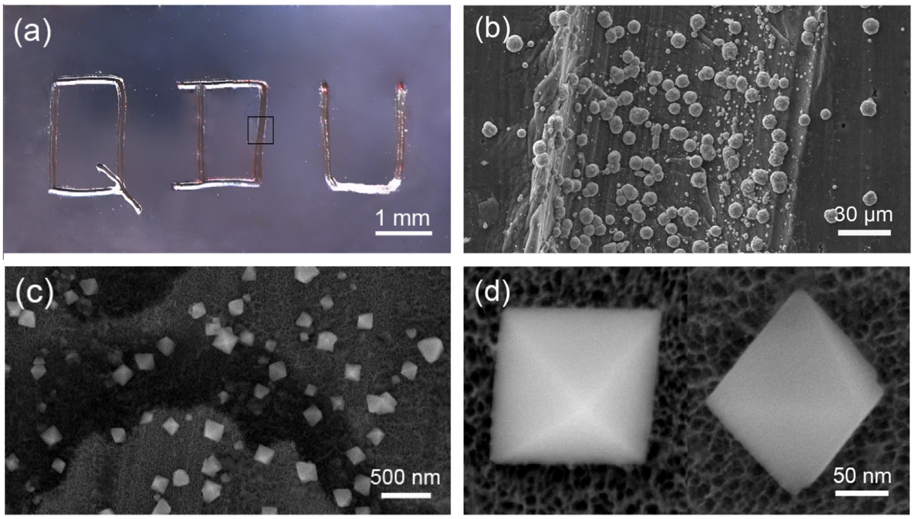

Figure 1. (a) Al foil with regular pattern after deposition; (b) SEM image of the region enclosed by a square in (a); (c) low-magnification SEM image of a part of (b); (d) enlarged SEM image of single Cu_2O nanooctahedra.

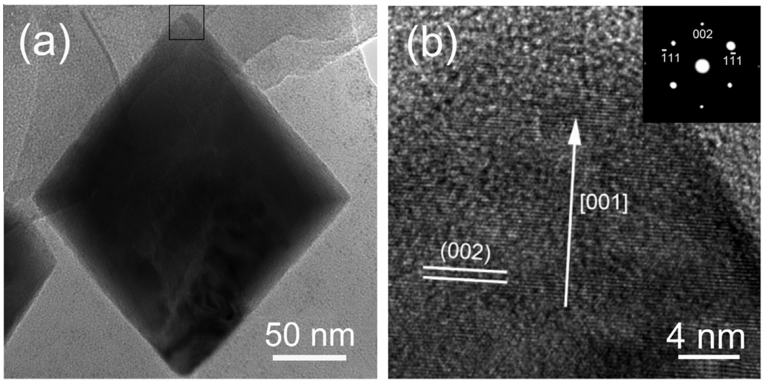

Figure 2. (a) Typical TEM image of a Cu_2O nanooctahedron; (b) Typical HRTEM image of the region enclosed by a square in (a) and corresponding SAED pattern.

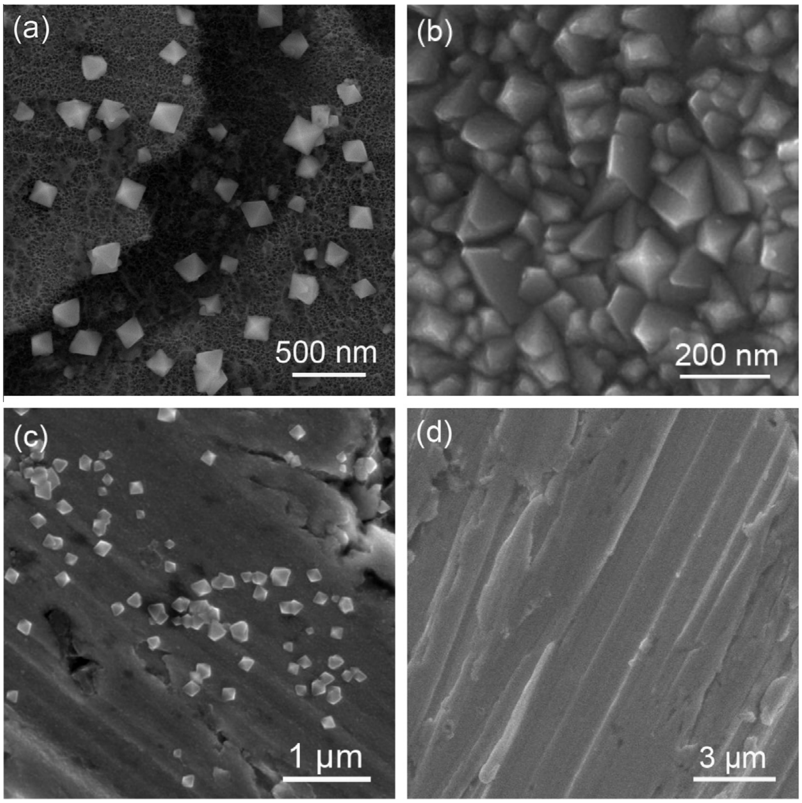

Figure 3. SEM images of the products deposited on different substrates. (a) Al, (b) Fe, (c) Cu, (d) Pt.

that the Al oxide film cannot be dissolved by NaOH, an Al foil without scratches on its surface was applied as the substrate and no Cu_2O nanocrystals formed. Based on the above analysis, we conclude that Cu_2O can be synthesized by electrodeless deposition only when the reducibility of metal substrates is more active than that of Cu. The reducibility of metal is the determining factor for the electrodeless deposition.

A possible growth mechanism is proposed for electrodeless deposition of Cu_2O nanooctahedra, as shown in Figure 4. The formation of Cu_2O nanooctahedra is attributed to the synergic effect of the reduction of Cu^{2+} by the metal and surface selective adsorption. In the solution, Cu^{2+} complexing with LA forms two kinds of complexes, CuL_2^{2-} and $[CuL_2(OH)]^{3-}$. At first, CuL_2^{2-} ion dominates in the acidic solution. As NaOH solution is added dropwise, the OH^- concentration increases, and the complex compound changes into $[CuL_2(OH)]^{3-}$ [19,20]. This is consistent with the gradual change of the solution color observed. Then, the complex reacts with metal substrates and Cu_2O nanooctahedra form because of the selective adsorption effect of LA. The polarized functional group '–C=O' in lactate ions with a negative charge prefers to interact with positively-charged 'Cu' in order to balance the local charge. It is the {1 1 1} planes that have the active coordination unsaturated 'Cu' so the lactate ions could be adsorbed primarily

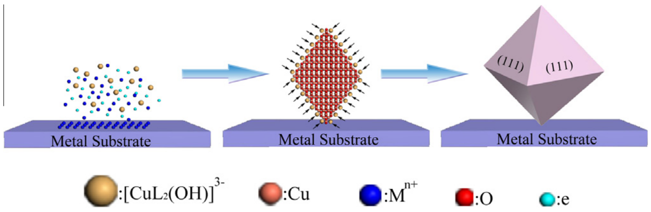

Figure 4. Schematic diagram for the formation mechanism of Cu_2O nanooctahedra.

on the {1 1 1} planes. The possible chemical reactions are as follows:

$$Cu^{2+} + 2L^{2-} \rightarrow CuL^{2-}$$

$$CuL_2^{2-} + OH^- \rightarrow [CuL_2(OH)]^{3-}$$

$$2n[CuL_2(OH)]^{3-} + 2M \xrightarrow{60\,^\circ C} nCu_2O\downarrow + nH_2O + 4nL^{2-} + 2M^{n+}$$

Usually, the reduction reaction is completed in a split second which may cause all the Cu_2O nuclei to gather together and form one big aggregation instead of many monodispersed Cu_2O nanooctahedra. It is known that the copper ions exist as the complex in the solution and it decomposes slowly as the Cu^{2+} ions are depleted. In our experiments, this could decrease the reaction rate. Moreover, when the aggregation becomes large enough, the concentration of the complex decreases and the concentration of L^- increases so that the growth of aggregations is limited further. That is why so many small aggregations and monodispersed Cu_2O nanooctahedra are produced.

Cu_2O nanooctahedra formed on Al substrates have narrow dimension distribution and were selected for the photocatalytic study. The UV–vis absorption spectrum of Cu_2O nanooctahedra is shown in Figure 5a. The spectral features are similar to those reported before [21,22]. Broad absorption bands dominate in the absorption spectrum, covering a wide range from visible light to the near-infrared region for Cu_2O nanooctahedra. Intrinsic band gap absorption can still be observed for the samples in the range from 400 to 700 nm, but the bands are generally weak. The optical band gap is obtained using the following equation [22] for a semiconductor:

$$\alpha h\nu = K(h\nu - E_g)^{n/2} \qquad (1)$$

where α is the absorbance coefficient, K is a constant, and n equals to 1 for direct transition and 2 for indirect transition. A plot of $(\alpha E_{photon})^2$ vs. the energy (E_{photon}) of absorbed light gives the band gap of Cu_2O nanooctahedra as shown in Figure 5b. The extrapolated value (the straight line to the X-axis) of E_{photon} at $\alpha = 0$ gives an absorption edge energy (called the band gap), $E_g = 2.31$ eV, which is in the visible light region. This value is a little larger than the direct band gap (2.17 eV) of bulk Cu_2O possibly because of the quantum size effect [23].

Cu_2O has been used as a good visible light photocatalyst due to its narrow energy band. Degradation of MO was used to evaluate the photocatalytic activity of the Cu_2O nanooctahedra. Figure 6 shows the absorbance of MO with Cu_2O nanooctahedra versus wavelength of UV light. From Figure 6 two curves can be seen, one being a solid curve for the solution without visible light irradiation and the other being a dashed line for the solution under visible light. The absorbance peak value of the solution under visible light is much lower than that of the samples without visible light irradiation. The absorbance peak value for the solution without visible light irradiation is 1.319 and the peak value for those under visible light is 0.269 at a wavelength of 465 nm. Meanwhile, the blank Al foils were immersed into MO solution as a reference. The UV–vis absorption spectrum is consistent with the absorbance peak value of the solution without visible light irradiation. The result above confirmed that MO was degraded by Cu_2O nanooctahedra. The photocatalytic efficiency (η) can be calculated from the peak values according to the following equation [24]:

$$\eta = \frac{A_0 - A}{A_0} \times 100\% \qquad (2)$$

In Eq. (2), A_0 and A are the absorbance peak values of MO with Cu_2O nanooctahedra without visible light and under visible light for 3 h, respectively. Based on the experimental results, the photocatalytic efficiency was calculated to be 79.60% according to Eq. (2), which is similar to the results reported by Zhang et al. under the same experimental conditions [9].

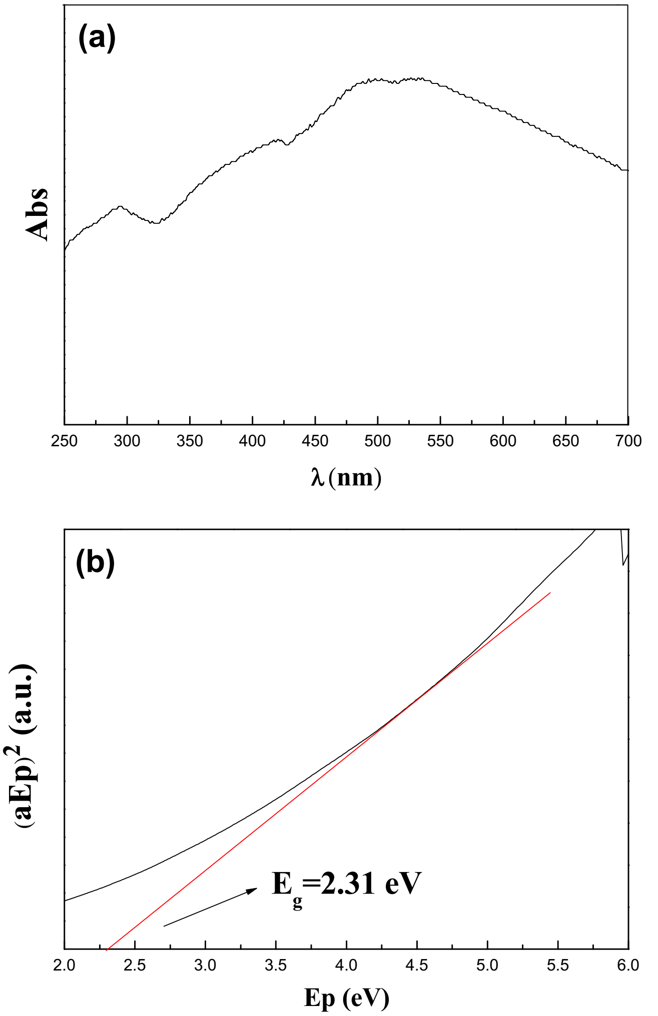

Figure 5. UV–vis absorption spectrum of Cu_2O nanooctahedra (a) and bandgap evaluation from the plots of $(\alpha E_{photon})^2$ vs. E_{photon} (b).

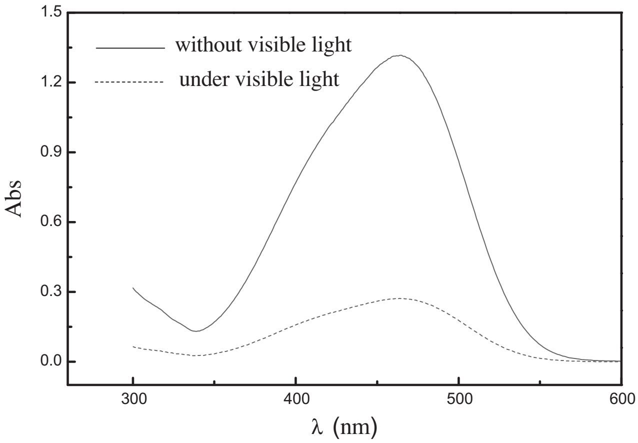

Figure 6. UV–vis spectra of MO with Cu_2O nanooctahedra, the solid curve showing the absorbance value of the samples without visible light irradiation and the dashed line for the samples under visible light.

4. Conclusions

In summary, well-faceted Cu_2O nanooctahedra with an average edge length of 150 nm have been fabricated by electrodeless deposition method for the first time. The formation of Cu_2O nanooctahedra is attributed to the synergic effect of redox reaction between Cu^{2+} with metal substrates and surface selective adsorption. Moreover, Cu_2O nanocrystals will form only when the reducibility of metal substrate is more active than that of Cu. Cu_2O nanooctahedra shows an excellent photocatalytic activity in the degradation of MO which may provide guidance for its application in the treatment of organic pollutants.

Acknowledgements

The authors would like to acknowledge the financial support from National Key Basic Research Development Program of China (973 special preliminary study plan) (Grant No. 2012CB722705), the Natural Science Foundation for Outstanding Young Scientists in Shandong Province, China (Grant No. JQ201002), the Scientific Research Award for Outstanding Young and Middle-Aged Scientists in Shandong Province (Grant No. BS2009CL0005), the Program for High Education Science and Technology in Shandong Province (Grant No. J12LA17), the Program for Foreign Cultural and Educational Experts (Grant No. W20123702083), the Scientific Research Starting Foundation for Introduced Talents at Qingdao University (Grant No. 06300701), and the Taishan Outstanding Overseas Scholar Program of Shandong Province, China.

References

[1] F.Y. Wang, Q.D. Yang, G. Xu, N.Y. Lei, Y.K. Tsang, N.B. Wong, J.C. Ho, Nanoscale 3 (2011) 3269.
[2] G.S. Shao, F.Y. Wang, T.Z. Ren, Y.P. Liu, Z.Y. Yuan, Appl. Catal. B 92 (2009) 61.
[3] K. Akimoto, S. Ishizuka, M. Yanagita, Y. Nawa, G.K. Paul, T. Sakurai, Sol. Energy 80 (2006) 715.
[4] X.D. Liang, L. Gao, S.W. Yang, J. Sun, Adv. Mater. 21 (2009) 2068.
[5] R. Liu, E.A. Kulp, F. Oba, E.W. Bohannan, F. Ernst, J.A. Switzer, Chem. Mater. 17 (2005) 725.
[6] Y.B. Cao, J.M. Fan, L.Y. Bai, F.L. Yuan, Y.F. Chen, Cryst. Growth Des. 10 (2010) 232.
[7] J.S. Bradley, B. Tesche, W. Busser, M. Maase, J. Am. Chem. Soc. 122 (2000) 4631.
[8] Y.J. Xiong, B.J. Wiley, Y.N. Xia, Angew. Chem. Int. Ed. 46 (2007) 7157.
[9] Y. Zhang, B. Deng, T.R. Zhang, D.M. Gao, A.W. Xu, J. Phys. Chem. C 114 (2010) 5073.
[10] H.L. Xu, W.Z. Wang, W. Zhu, J. Phys. Chem. B 110 (2006) 13833.
[11] Y.J. Xiong, Z.Q. Li, R. Zhang, Y. Xie, J. Yang, C.Z. Wu, J. Phys. Chem. B 107 (2003) 3697.
[12] Y. Chang, H.C. Zeng, Cryst. Growth Des. 4 (2004) 273.
[13] Z.W. Pan, Z.R. Dai, Z.L. Wang, Science 291 (2001) 1947.
[14] Y.Q. Wang, W.S. Liang, A. Satti, K. Nikitin, J. Cryst. Growth 312 (2010) 1605.
[15] S.J. Guo, Y.X. Fang, S.J. Dong, E.K. Wang, Inorg. Chem. 46 (2007) 9537.
[16] B.X. Li, X.F. Wang, D.D. Xia, Q.X. Chu, X.Y. Liu, F.G. Lu, X.D. Zhao, J. Solid State Chem. 184 (2011) 2097.
[17] S.Y. Jing, S.X. Xing, Y. Wu, Y.F. Wang, B. Zhao, C. Zhao, Mater. Lett. 61 (2007) 2281.
[18] H.B. Michaelson, J. Appl. Phys. 48 (1977) 4729.
[19] S. Leopold, M. Herranen, J.O. Carlsson, L. Nyholm, J. Electroanal. Chem. 574 (2003) 49.
[20] K.D. Singh, S.C. Jain, T.D. Sakore, A.B. Biswas, Z. Kristallogr. 141 (1975) 473.
[21] K.H. Chun, C.H. Chen, M.H. Huang, Adv. Funct. Mater. 17 (2007) 3778.
[22] C.H. Bernard, W.Y. Fan, J. Phys. Chem. B 110 (2006) 20805.
[23] D.P. Singh, N.R. Neti, A.S.K. Sinha, O.N. Srivastava, J. Phys. Chem. C 111 (2007) 1643.
[24] C.Y. Li, J.B. Wang, Y.Q. Wang, Chin. Phys. B 21 (2012) 098102.